

We are IntechOpen, the world's leading publisher of Open Access books Built by scientists, for scientists

6,900

Open access books available

186,000

International authors and editors

200M

Downloads

Our authors are among the

154

Countries delivered to

TOP 1%

most cited scientists

12.2%

Contributors from top 500 universities



WEB OF SCIENCE™

Selection of our books indexed in the Book Citation Index
in Web of Science™ Core Collection (BKCI)

Interested in publishing with us?
Contact book.department@intechopen.com

Numbers displayed above are based on latest data collected.
For more information visit www.intechopen.com



Time Critical Mass Evacuation Simulation Combining A Multi-Agent System and High-Performance Computing

Leonel Aguilar, Maddegedara Lalith and
Muneo Hori

Additional information is available at the end of the chapter

<http://dx.doi.org/10.5772/intechopen.69844>

Abstract

This chapter presents an application of multi-agent systems to simulate tsunami-triggered mass evacuations of large urban areas. The main objective is to quantitatively evaluate various strategies to accelerate evacuation in case of a tsunami with a short arrival time, taking most influential factors into account. Considering the large number of lives in fatal danger, instead of widely used simple agents in 1D networks, we use a high-resolution model of environment and complex agents so that wide range of influencing factors can be taken into account. A brief description of the multi-agent system is provided using a mathematical framework as means to easily and unambiguously refer to the main components of the system. The environment of the multi-agent system, which mimics the physical world of evacuees, is modelled as a hybrid of a high-resolution grid and a graph connecting traversable spaces. This hybrid of raster and vector data structures enables modelling large domain in a scalable manner. The agents, which mimic the heterogeneous crowd of evacuees, are composed of different combinations of basic constituent functions for modelling interaction with each other and environment, decision-making, etc. The results of tuning and validating of constituent functions for pedestrian-pedestrian, car-car and car-pedestrian interactions are presented. A scalable high-performance computing (HPC) extension to address the high-computational demand of complex agents and high-resolution model of environment is briefly explained. Finally, demonstrative applications that highlight the need for including sub-meter details in the environment, different modes of evacuation and behavioural differences are presented.

Keywords: tsunami-triggered mass evacuation, multi-agent system, mixed mode evacuation, parameter tuning, high-performance computing

1. Introduction

There are several advantages of applying multi-agent systems to study mass evacuations like those triggered by mega tsunamis. Undoubtedly, the widely used simple methods like 1D-networks and queue models for simulating mass evacuation are quite useful in disaster mitigation efforts. However, they have many limitations. Considering the number of human lives in fatal danger, it is of great interest to use more sophisticated models which are close-to-reality models of environments and agents which can mimic evacuees' behaviours of significance. Unlike widely used 1D-networks or queues, multi-agent systems provide a great flexibility in the level of sophistication and allow one to gradually develop a close-to-reality model.

Details of a multi-agent system developed for simulating tsunami-triggered mass evacuation in large coastal regions are presented in this chapter. The multi-agent system is developed with the aim of including a sub-meter resolution model of the environment including the interior of buildings, dynamic changes in the environment, etc., and agents capable of perceiving this environment as evacuees do and mimic evacuees' behaviours of significance. It is essential to utilize high-performance computing (HPC) resources like computer clusters to meet the significantly high-computational demand of such multi-agent systems. A scalable HPC extension is included in the developed system so that an area of several hundreds of square kilometres with millions of agents can be simulated. The amount of computations involved should not be a great concern in developing such multi-agent systems. The rapid progress of HPC technologies will enable one to do sophisticated and large scale simulations on a workstation class computer, within few decades.

The rest of the chapter is structured as follows. Section 2 discusses a mathematical framework for the specification of multi-agent systems. Section 3 details the multi-agent system including the evacuee modelling features and the techniques for efficient modelling of environments. Parallel computing extension to efficiently utilize HPC resources is briefly presented in Section 4. Section 5 presents the validation of the model. Finally, Section 6 provides demonstrative examples showing the necessity of such models.

2. Framework

The multi-agent system is specified using a mathematical framework adapted from the field of dynamical systems, see [1] for further details. This section provides generic definitions for an agent, agent's local system, and the multi-agent system as a dynamical system. The purpose of this section is to provide a clear language to refer to the different parts and properties of the system.

Let the i th agent, a_i , be defined as a collection $a_i = \{s_i, f_i\}$, where s_i represents the agent's state and f_i its local update function. The local update function f_i encompasses all the possible actions, interactions, behaviours and thought processes an agent can exhibit. On a system with n agents, the set of all agents is given by $A = \{a_i \mid i = 1, \dots, n\}$. The state s_i is further composed by two sub-states $s_i = \{s_i^{int}, s_i^{ext}\}$. s_i^{int} is the agent's internal state which holds the information that

would not be available to other agents without explicit communication (e.g. gathered experiences, final destination). In contrast, the agent's external state s_i^{ext} contains information inferable by to other agents without explicit communication (e.g. speed, moving direction, etc.).

For every agent a local system is defined which captures the individual effects of the agent on its neighbourhood. Agent a_i 's neighbourhood N_i is composed by its visible physical surrounding, N_i^{env} , and a set of agents it can interact with, N_i^{agent} ; $N_i = \{N_i^{env}, N_i^{agent}\}$ and $N_i^{env} \subset E$, where E denotes the whole environment. The discrete time evolution of an agent's local system state $x_i = \{s_i, N_i\}$ due to the agent's actions is defined by $x_i^{t+\Delta t} = f_i(x_i^t)$. Actions of each individual agent make the multi-agent system to evolve from state $\{x_i^t \mid i = 1, \dots, n\}$ to $\{x_i^{t+\Delta t} \mid i = 1, \dots, n\}$.

In addition to the agents' actions, the changes in the environment due to natural causes like earthquakes, tsunami, etc. are modelled by applying environment update functions $\Lambda = \{\lambda_j \mid j = 1, \dots, m\}$ in appropriate order.

The multi-agent system is conceptualized as a parallel discrete dynamical system. In this system next state is independent of the order of execution of the agents, and only depends on the former state. Temporary copies of the agent states are used to preserve the properties of the parallel dynamical system. The time evolution of the whole system is defined by updating of the environment followed by updating of all the n number of agents, as follows.

$$\begin{aligned} E^{t+\Delta t} &= (\lambda_1 \circ \lambda_2 \dots \circ \lambda_m)(E^t) \\ x_i^{t+\Delta t} &= f_i(x_i^t) \text{ for } i = 1, \dots, n \end{aligned} \tag{1}$$

3. The multi-agent system

As customary to most multi-agent systems, an agent system for evacuation simulation is also composed of two main components: agents and environment. The agents model the evacuees, while the environment provides the physical context in which the evacuation happens. This section provides an overview on the models of agents and environment.

3.1. Agents

Agents are composed by combining elementary functions that enable them to perceive their visible surroundings, take decisions based on their previous knowledge and current experiences, navigate in dynamically changing environment updating their memory, etc.

The logic to model evacuees' possible actions, interactions, behaviours, thought processes, etc. is embedded in the agent's local update function f_i . Local update functions, f_i , are built through the composition of basic constituent functions g^j 's, $f_i = g^1 \circ g^2 \dots \circ g^p$. These constituent functions include elementary functions that enable agents to perceive their visible surroundings, take decisions based on their previous knowledge and current experiences, navigate in dynamically changing environment updating their memory, etc. Brief descriptions of some of the implemented constituent functions are given below.

g^{eye} : scans N_i^{env} and creates a boundary of visibility in s_i^{int} according to a_i 's eye sight.

$g^{find_way_out}$: analyzes the boundary of visibility and identifies ways out in the visible neighbourhood.

$g_{pedestrians}^{navigate}, g_{cars}^{navigate}$: defines the way pedestrians and vehicles navigate through the environment given the available information.

$g^{find_interact}$ finds agents to interact with, based on visibility, interaction radius, etc.

g^{coll_av} : finds a collision free velocity to move along the path chosen in $g^{navigate}$, evading collision with neighbours identified with g^{find_inter} it is based on Optimal Reciprocal Collision Avoidance (ORCA) [2].

g^{path_plan} : finds paths to a suitable destination, satisfying desired requirements like shortest, perceived to be safest, etc., taking any past experiences into account [1].

$g^{is_path_blocked}$: visually identifies whether a current path is blocked.

$g^{find_a_followee}$: finds an agent to be followed.

$g^{follow_an_agent}$: follows any agent identified with $g^{find_a_followee}$.

$g^{seek_not_evacuating}$: seeks for agents who have not started to evacuate.

$g^{order_to_evacuate}$: orders an agent, identified with $g^{seek_not_evacuating}$, to start evacuation immediately.

$g^{execute_an_action}$: executes a desired action such as move.

g^{update} : updates an agent's state.

The heterogeneity inherent of human crowds can be modelled by changing the agents' properties or by changing its logic. The components in each agent's state, s_i can be varied and assigned based on observed data. Properties like speed are drawn from observed distributions within a valid range for each age group. Agents belonging to the same age group are instantiated using the same distributions for their parameters. Different combinations of the constituent functions give rise to different behavioural models. For practical reasons, only a small set of local update functions are defined to represent the major roles and aspects of interest in the evacuation; $\{f^\tau\} = \{f^{resident}, f^{visitor}, f^{car}, \dots\}$ where τ represents the different agent types.

3.2. Specialized agent types — a^τ

The functionality provided by the different constituent functions can be separated into three main groups pertaining to human actions; *see*, *think* and *act*. *See* contains constitutive functions related to the acquisition of the information of the surroundings, *think* provides functions related to the cognition and decision-making, and finally *act* executes the decisions, actions and interactions chosen by the agent. Different behavioural models are created by specializing *think* with different constituent functions. As the focus of the evacuation simulator is on the evacuees' movement, the main way of interaction happens through the collision avoidance.

To exemplify different modes of evacuation and behavioural models this chapter demonstrates the usability of the simulator using cars and pedestrians. Pedestrians are further subdivided in residents, visitors all of them provided with different information, and abilities.

Residents agents are used to model people familiar with the surroundings. They are able to use their knowledge to plan their path to the nearest evacuation area. **Figure 1** provides a sketch off the implementation of a resident agent, $f^{resident}$. Resident's *think* is composed by $g^{find_way_out}$, $g^{navigate}$, g^{find_inter} and g^{coll_av} . *Act* is composed of $g^{execute_actions}$ and g^{update} . s^{int} is provided with a topological map of the environment, which is used for gathering past experiences, planning paths with desired constraints, etc.

Visitor agents are used to model people unfamiliar with their surroundings. They navigate using the information they acquire through their vision and the experiences they collect while evacuating. They perceive the details of the surroundings with g^{eye} and $g^{identify_env}$. They seek a visible safe place like high grounds or follow other evacuees using $g^{follow_an_agent}$ in order to evacuate. Visitors can dynamically build their own mental maps as they explore the area and collect experiences.

Other agent types such as official agents that model figures of authority such as law enforcement, event staff, etc. are implemented. Their role is to help in the evacuation of other agents. They possess full information of the state of the environment and are assumed to be able to communicate with each other and collectively plan their actions.

Cars model a different mode of evacuation. They differ from pedestrians in the way they navigate and avoid collisions with each other and the pedestrians. While pedestrians are able to use the walkways or roads, cars movements are restricted to the road lanes. Cars are able to identify intersections. Due to the complexity of the intersections a simple queue model is used to model the effect of the intersections. Cars are able to recognize multi and single road lanes and use them accordingly. Cars are have access to the information of the environment and are able to plan their paths accordingly.

3.3. Environment—E

The environment provides the physical context in which the evacuation is happening. Formally the active environment is given by the union of all local neighbourhoods, $E^* = \bigcup_{i=1}^n N_i^{env}$. Although, $E^* \subset E$, for practical purposes they will be referred without distinction.

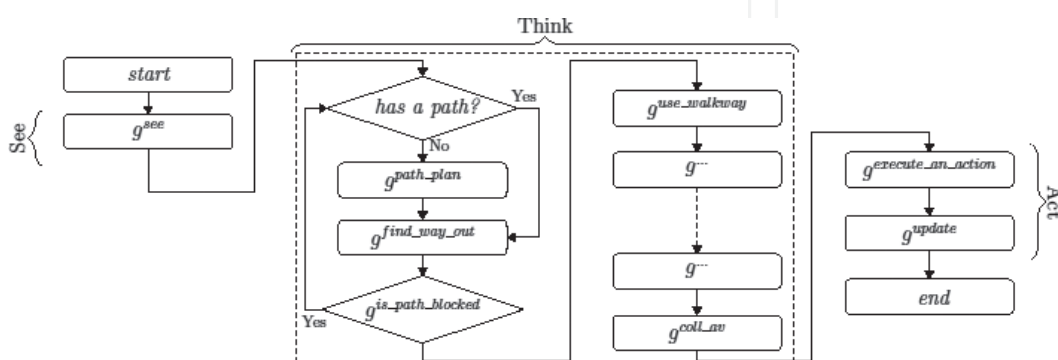


Figure 1. A simplified version of local system update function of the resident agents, $f^{resident}$.

Agents move in a continuous 2D space defined by walkable areas and roads. A hybrid model of environment consisting of raster and vector data is used to include the details of the physical environment and restrict the agents' movements, see **Figure 2**. Details of the empty spaces, obstacles, inundated areas and safe evacuation areas are provided by a grid, currently using resolutions of $1\text{ m} \times 1\text{ m}$ cells. Agents are able to perceive these details visually and incorporate information such as blocked paths to their experiences. The topological abstraction of the traversable spaces is represented with a graph. This graph is static and represents the agent's knowledge of the undamaged domain before the start of the evacuation. The use of raster and vector data enable the efficient representation of details (grid) and efficient execution of cognitive tasks involving past experiences (graph). As an example, in large domains of several square kilometres, path planning on the graph is several orders of magnitudes faster compared to that of grid. In contrast to other large scale evacuation simulators the environment provides perceivable information and obstacles, but it does not provide an explicit constraint on the movement based on the model resolution. For example, different cell sizes, or graph connectivity can provide more or less information but do not explicitly constrain the movement of the agents in contrast to cellular automata models, graph and queuing models commonly used in other large scale evacuation simulators.

Changes in the environment, λ_f , are included by coupling the evacuation simulator with other simulators. $\lambda_{\text{earthquake}}$ includes damage models based on the results of a seismic response analysis tool. **Figure 3** provides a sketch of the integration with the seismic response analysis and the evacuation simulator.

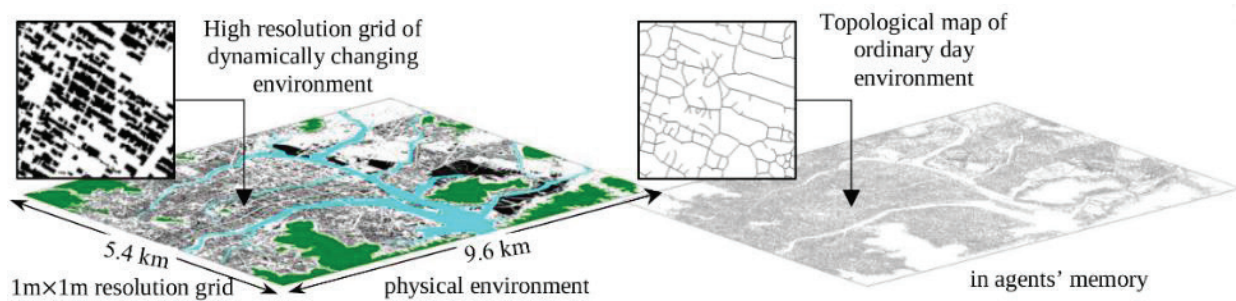


Figure 2. Hybrid model of the environment consisting of a high-resolution grid and topological graph. Grid is dynamically updated according to the changes in the environment. The graph is static and represents the path network before the disaster.

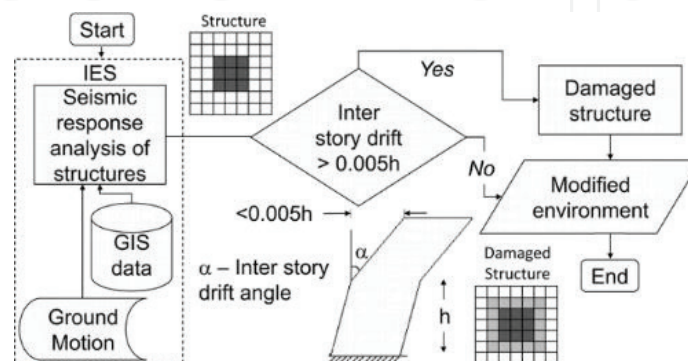


Figure 3. Integration of the seismic response analysis damage models with the evacuation simulator.

Additionally, $\lambda_{tsunami}$ provides information about the state of the inundated spaces due to tsunami. This information is provided by a tsunami inundation simulator with updates in 10 min intervals, see **Figure 4**.

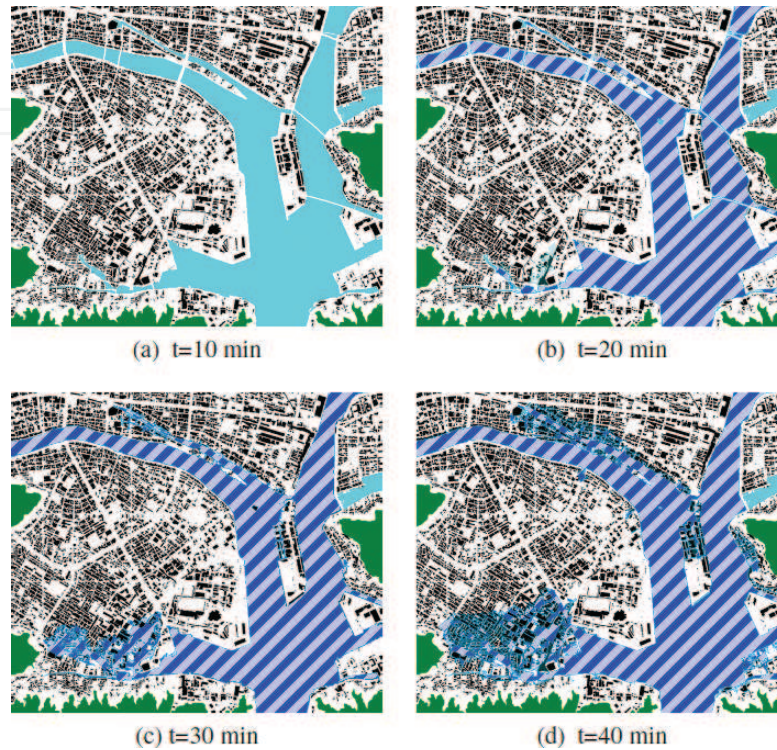


Figure 4. Snapshots of the tsunami inundation. Normal water level in cyan, inundated water level in blue (hatched).

4. Validating the model

One of the major challenges for the simulation of evacuations is providing confidence in the model. It has to be shown that the model is able to capture the essential characteristics of the evacuation (validation) and that the results are due to the emergence from those characteristics and not the result of an artefact in the simulation (verification). The validation of evacuation simulators is an area that requires further study and more and better techniques to provide the desired confidence.

This section provides an overview about the ongoing validation process. This first stage on validating the model is based on tuning the agents' interactions, specifically their collision avoidance with field observations and showing that after the tuning process the agents are capable to reproduce these observed results. This section is intended to provide a general idea of the validation process, for details on the parameters governing the interactions and the resulting values from the tuning process please refer to Ref. [3].

The pedestrian-pedestrian interaction is validated by re-enacting observations in [4] in the simulator. Monte Carlo simulations are performed varying the initial pedestrian densities

and obtaining 100 samples for each in a one directional pedestrian flow. **Figure 5** shows the results of comparing the simulations results (whisker box plots with outliers) with the regression over the data [4].

A similar procedure is performed with the car agents, their characteristics are tuned with data obtained in field observations in the Lincoln tunnel [5] and the results are plotted against these observations, see **Figure 6**.

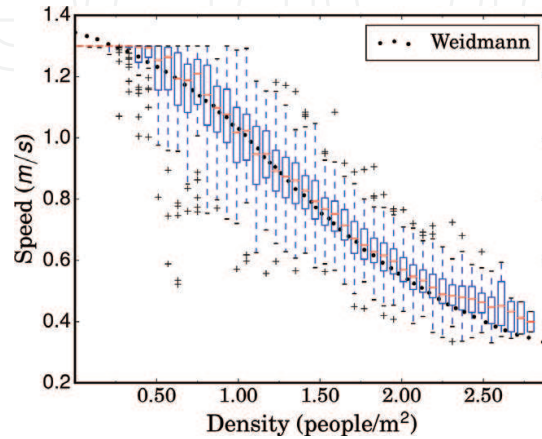


Figure 5. Comparison between simulation results and field observations for the pedestrian-pedestrian interaction.

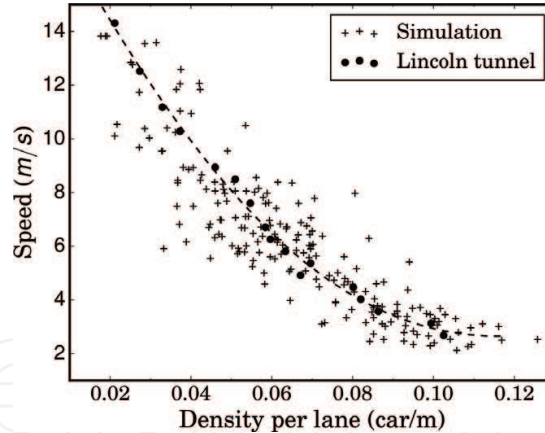


Figure 6. Comparison between simulation results and field observations for the car-car interaction.

Finally, the interactions between cars and pedestrians are validated. For these observations of cars and pedestrians interactions in Tokyo are recorded using a camera and quantified by hand frame by frame. These observations involved cars moving through crowds of pedestrians. The quantities are the cumulative amount of pedestrians in a square region in front of the car and the time it took the car to cross the study area, dividing the study area length by this time is what is referenced as the average flux speed. **Figure 7** shows the results of the tuning of parameters and the comparison of the simulation results with the field observations.

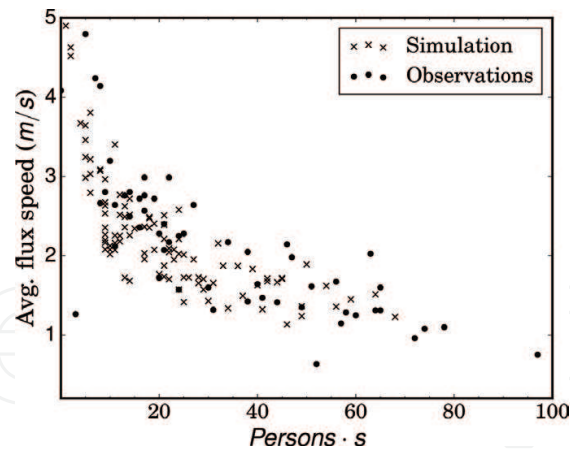


Figure 7. Comparison between simulation results and field observations for the car-pedestrian interaction.

Further parts of the evacuation simulator should be validated and verified, for example, reproducing macroscopic fundamental diagrams extracted from mobility data from cell phones.

5. Parallel computing extension

As the simulator possess the ability to model and evaluate a large number complex and heterogeneous evacuees in environments with sub-meter details the resulting high-computational load needs to be considered. The evacuation simulator takes advantage of high-performance computing (HPC) infrastructure consisting of computing nodes containing several CPU cores sharing memory within a node. These nodes are interconnected through a high-speed network.

To take advantage of the HPC infrastructure the simulation needs to be segmented in smaller pieces that can be dealt by individual computing nodes. For this purpose the environment, E , gets divided into rectangles and the information about the evacuees currently in that area is what is henceforth referred as a partition of the domain.

Hybrid parallelism using Message Passing Interface (MPI) and Open Multi-Processing (OpenMP) is used to create the parallel framework [6]. MPI messages are used to communicate the information between computing nodes and OpenMP is used to thread parallelize the execution of the agents within a partition considering each agent's execution a task. A run-time weighted 2D-tree-based domain decomposition is used for determining the partitions in the domain, see Figure 8. The use of a runtime weighted KD-tree for the domain decomposition allows assigning approximately a similar execution load to each partition. The partitions are provided with a ghost layer around it that keeps track of agents in neighbouring partitions, this to ensure continuity and consistency in the simulations. The communication overhead is amortized by executing the agents whose information need to be exchanged first and overlap the communication with the execution of the agents whose information does not need to be exchanged [7].

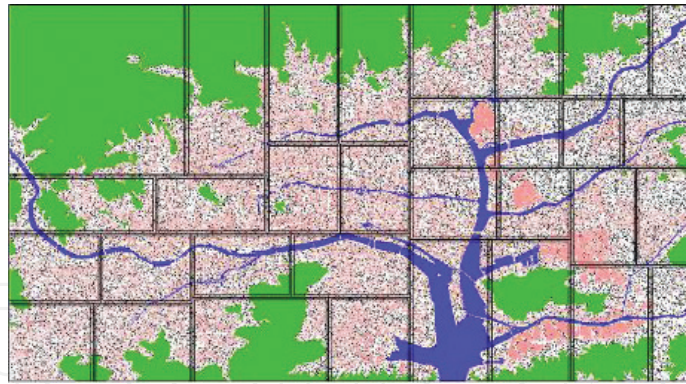


Figure 8. Domain decomposition example.

Intra and internode scalability is measured separately to evaluate how it degrades and where are the highest chances of improvement. Intra node scalability measures how the thread-parallel part (OpenMP) of the implementation degrades as the tasks of executing an agent are shared among a larger number of threads. The inter node scalability shows the performance of using flat-MPI as the number of processes (and partitions) increases. The intra-node scalability is tested using 100,000 agents in Kochi City area for 4000 time-steps. Measures for intra-node scalability are taken using a single node in The University of Tokyo's FX10 system, 16-core SPARC64 IXfx processor with 32 GB of RAM in the computing node. The inter node scalability is tested using 2 million agents in an 81 km² area of Tokyo for 400 time-steps using RIKEN's K computer, 8-core SPARC64 VIIIfx processor with 16 GB of RAM per computing node using flat MPI. Figures 9 and 10 show a comparison with the ideal scalability.

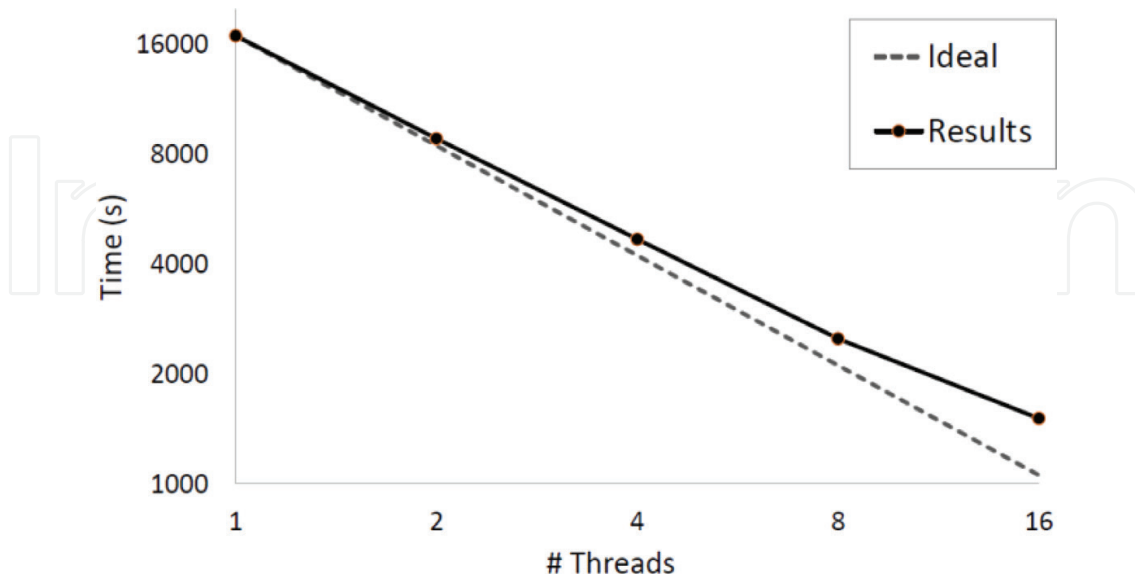


Figure 9. Intra node scalability.

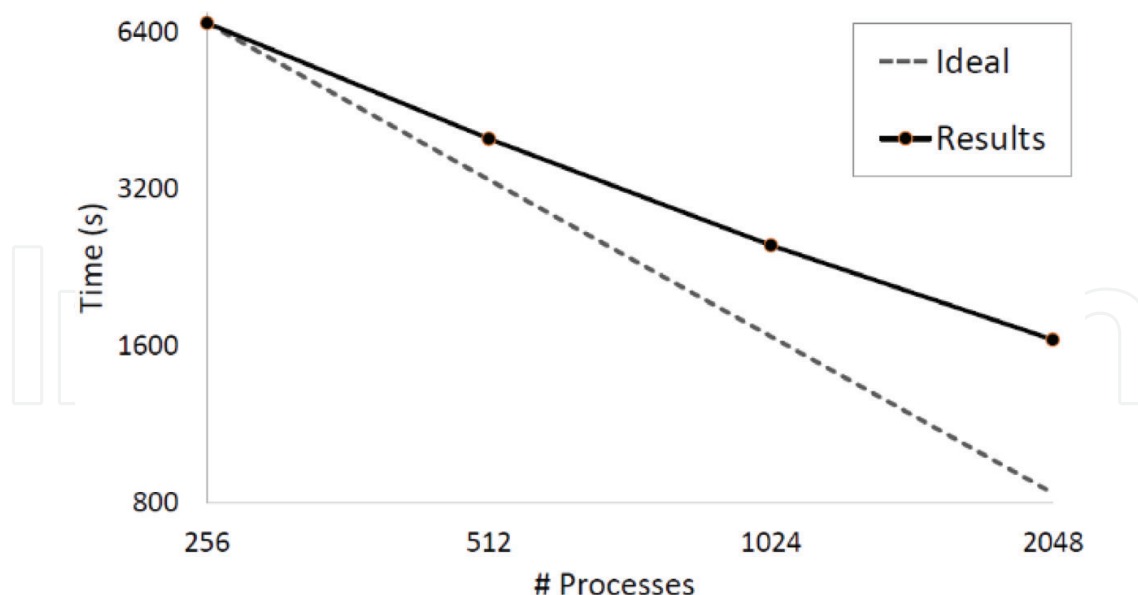


Figure 10. Inter node scalability.

6. Demonstrative examples

This section demonstrates the usage of the mass evacuation simulator it emphasizes the need of incorporating fine level details and mixed mode evacuations. For a proof of concept demonstration on the use of the evacuation simulator in an automatic evacuation management system see [8]. Some of the selected hypothetical scenarios demand a detailed model of environment, use of all available traversable area and complex agent functions, like the detection of blocked paths, navigation, etc. The ability to incorporate complex models of agents and details in the environment highlights the advantages over the simplified 1-D models. The purpose of these demonstrations is to show the capabilities of the simulator, they are not intended to provide reliable results. Providing reliable results would require a group of experts of different fields building and evaluating the behavioural models and assumptions about the evacuation.

The demonstrations are separated into two groups: pedestrian only and multi modal evacuation (pedestrian and cars). The robustness and variability of the scenarios in each category is evaluated through Monte Carlo simulations and converged results are provided for the relevant scenarios.

6.1. Pedestrian only scenarios

This section presents scenarios involving pedestrian only evacuations where changes in the environment, different evacuation behaviours and mitigation measures are tested to highlight the need of detailed modelling in mass evacuations and demonstrate the capability of

the software to evaluate scenarios in a quantitative manner. First evacuation during daytime is evaluated, then evacuation during night time and finally night time evacuation during a special event are contrasted.

6.1.1. Common settings

For the pedestrian only demonstrations, a coastal city located in the southern part of Honshu island of Japan is considered. This city was chosen as it has suffered from several historical tsunamis. The domain considered is $9.6 \times 5.4 \text{ km}^2$, in a $1 \text{ m} \times 1 \text{ m}$ resolution grid, see **Figure 11**. An evacuation involving 57,000 persons is assumed. The evacuees are divided into two age groups, below and above 50 years, and their properties are set according to **Table 1**. Regions with an elevation above 30 m, shown in green, are considered as the safe evacuation areas. Evacuation to nearby tall buildings is not considered since only a few tall buildings are available in this coastal city. All the areas not occupied by buildings or water bodies are considered traversable.

The earthquake induced damages, $\lambda_{\text{earthquake}}$ in the region are estimated using a physics based seismic response analysis simulator [9], with the strong ground motion of 1995 Kobe earthquake. The damage state of buildings are evaluated based on a simple standard criterion used in earthquake engineering; buildings are considered to be damaged if the inter-story drift angle is larger than 0.005 [10]. The occupied area is increased by 40% of the building height

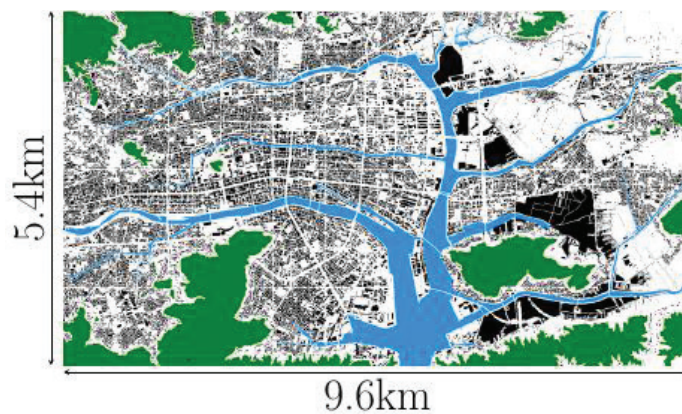


Figure 11. Environment for pedestrian only demonstrative examples.

	Younger than 50 years (55%)	Older than 50 years (45%)
Speed mean (m/s)	1.43	1.39
Speed S.D. (m/s)	0.11	0.19
Sight distance (m)	50	50
Pre-evacuation time mean (s)	1000	1000
Pre-evacuation time S.D. (s)	600	600

Table 1. Properties of the two age groups of agents for the pedestrian only scenarios.

[11], if a building is deemed damaged. The grid is updated every 5 min, according to [12], to mimic the tsunami inundation (i.e. $\lambda_{tsunami}$); the arrival time of the tsunami is 15 min.

6.1.2. Monte Carlo simulations

The results of simulations have a certain degree of uncertainty due to the presence of various random variables. In order to improve the reliability of the simulation results, taking the effects of these uncertainties into account, Monte Carlo simulations are conducted. The only random variables considered in the present simulations are the distribution of evacuees and their speeds.

To decide a sufficient number of simulations required for each Monte Carlo simulation, 1000 (=N) sets of evacuation simulations are conducted, and the convergence of standard deviation of an influential quantity with respect to the number of simulations n , $1 < n \leq N$, is analyzed. As for the settings, the 1000 simulations are composed of randomly generated agents' initial locations and speeds, while the scenario considered is evacuation to high grounds in the absence of earthquake disaster or tsunami inundation.

The standard deviation of the total number of agents evacuated after 40 min is considered as the influencing factor, in deciding the necessary number of simulations per Monte Carlo simulation, since total number of agents evacuated is one of the influential quantities. As shown in **Figure 12**, the standard deviation of the total number of people evacuated at 40 min converges (i.e. has negligibly low variation) for $n > 400$. In addition to the fore-mentioned global measure, statistical data of number of agents evacuated at each 30 s interval are compared as a local measure. **Figure 13** shows the mean number of agents evacuated at each 30 s interval, for the two cases with $n = 1000$ and $n = 400$. As is seen, both the cases have nearly identical mean values and standard deviations. Since both of above considered global and local measures have converged when $n > 400$, 400 is set to be the sufficient number of simulations for the convergence of Monte Carlo simulations. The value of sufficient n , depends on

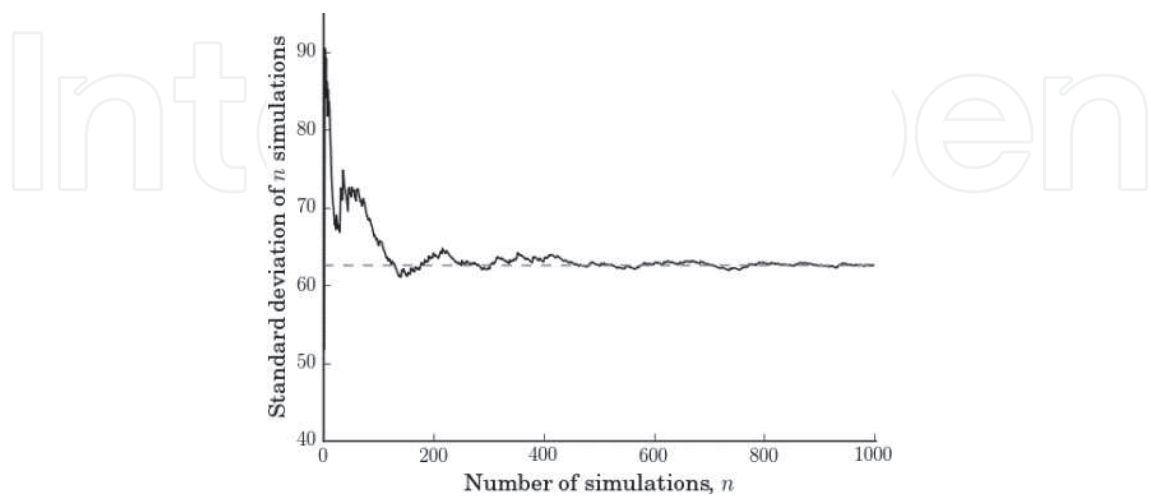


Figure 12. Standard deviation (S.D.) of cumulative number of agents evacuated by 40 min, from 2 to 1000 simulations.

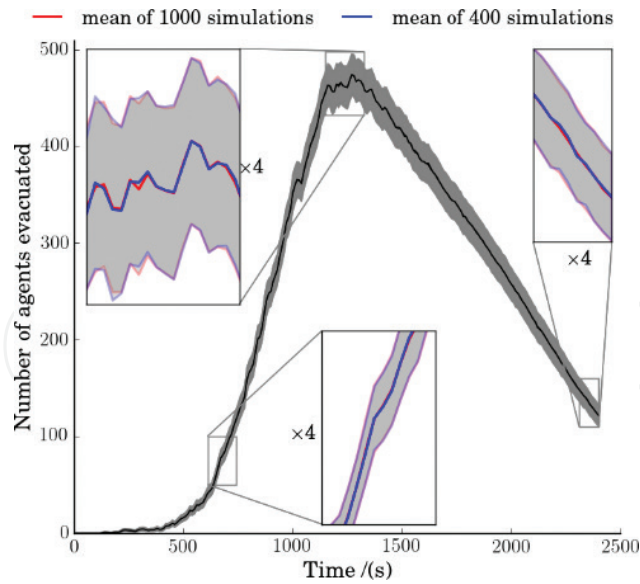


Figure 13. Mean number of agents evacuated at each 30 s intervals.

the number and the nature of the random variables considered, and the real applications may require a larger value.

6.1.3. Day time evacuation during an ordinary day

Under day time evacuation, four scenarios are considered; without any damages to the environment, with earthquake disaster; with tsunami inundation; and with both the earthquake damages and tsunami inundation. For all these cases, the 57,000 resident agents are considered, while they are positioned within 20 m proximity of buildings initially.

Figure 14 shows the time histories of cumulative number of agents evacuated for each of the four scenarios. As is seen, both the earthquake damages and tsunami inundation reduces the number of evacuees almost by the same amount. The effect of the tsunami inundation is mostly attributed to the inundation of a few critical bridges in the study area. Comparing the effect of manually blocking these bridges with the effect of the tsunami inundation shows similar results, see **Figure 15**.

However, while the effects of earthquake damages start to appear at early stages, the effect of tsunami inundation appears after 20 min; as the tsunami arrival time is 15 min.

6.1.4. Night time evacuation in an ordinary day

Due to various factors like low lighting conditions, being tired, sleepy, etc., evacuees tends to have different behaviours in night time evacuations, compared to those of day time; late to start evacuation, have slower walking speeds, may seek for safer routes, etc. The scenarios considered here aim to model mainly the effects of lower visibility and the tendency to take safer roads.

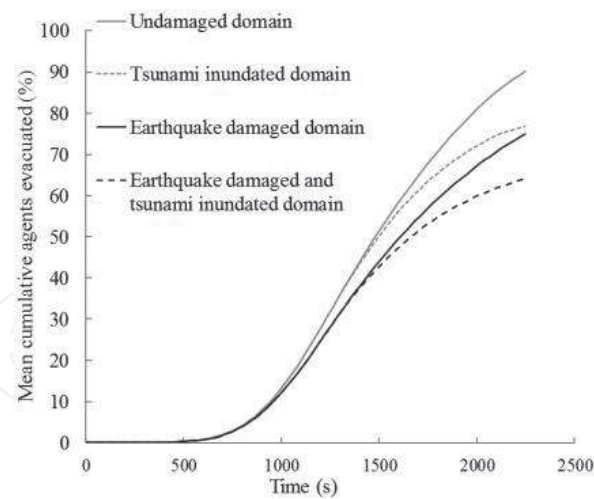


Figure 14. Time history of cumulative number of agents evacuated (mean of 400 simulations). Effect of environmental damage.

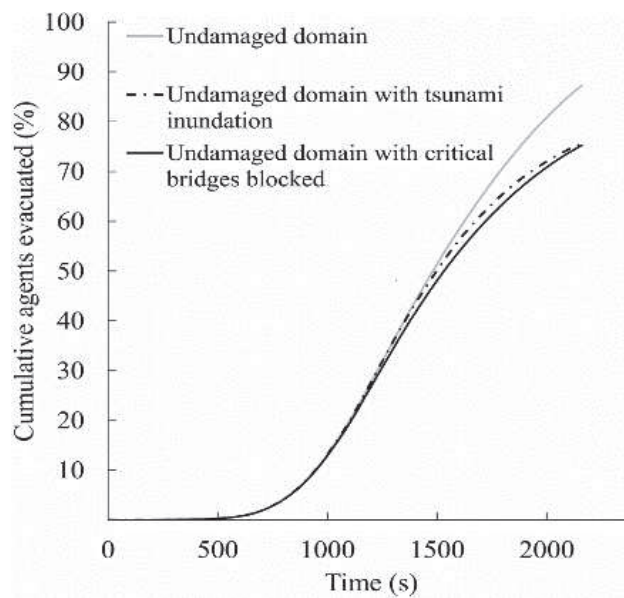


Figure 15. Time history of cumulative number of agents evacuated (mean of 400 simulations). Effect of damaged bridges.

It is assumed to be a full moon light and the earthquake has damaged the environment causing a complete power failure. Accordingly, agents' maximum sight distance is reduced to 15 m [13]. Due to the lack of information on the effect of lighting condition on the walking speed, the walking speed of the two groups of agents are set according to Table 2 [14]. The lower visibility not only lowers the walking speed, but also makes it slow the identifying of blocked roads; require making close examinations to confirm their paths are blocked.

When evacuating right after an earthquake, like the present scenario, people tend to take paths with longer stretches of wider roads to lower the probability of encountering blocked

Max visibility radius	Younger than 50 years (%)	Older than 50 years (%)
15 m visibility (0.2 lx)	70	50
30 m visibility with 15 lx	90.6	83

Table 2. Pedestrian speeds under different lighting conditions (the value is set as a percentage of their desired speed, for example, if the desired speed is 1 m/s the modified desired speed is set to 0.5 m/s if the agent is older than 50 years old and under 0.2 lux lighting condition).

roads, depending on the intensity of ground shaking they experienced. The standard path planning algorithms like Dijkstra algorithm allow the use of strong constraints like the minimum width of a road, etc. However, the present scenario requires weaker constraint to find paths with longer stretches of wider roads as far as possible, while strictly satisfying strong constraints on total time or/and distance. As an example, an evacuee may prefer to take wider roads or avoid narrow roads as far as possible, and while ensuring to reach a safe place before the tsunami arrives. In order to include such weak constraints, the standard Dijkstra algorithm is slightly modified [1] by introducing two distance measures; the actual distance, and a perceived distance. When estimating the perceived distance, the roads wider than the preferred width are reduced in length according to the level of preference.

Figure 16 compares the ordinary day time evacuation with that of night time with and without the effects of earthquake and tsunami. As is seen, there is nearly 30% reduction in number of evacuees between the day and night scenarios without earthquake and tsunami effects. The damages in the environment further reduce the number of evacuees by almost 8%, at the end of 40 min. These results highlight the ability of the developed system to take different influencing factors like lighting conditions and the preference of safer roads.

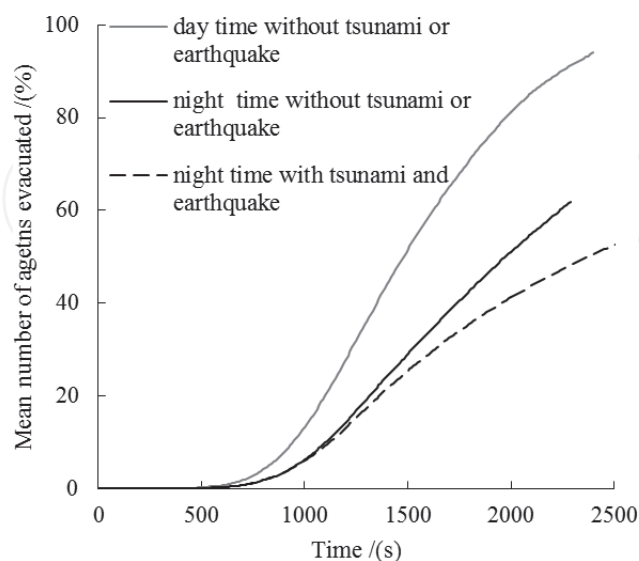


Figure 16. Time histories of total number of evacuated agents for day time and night time evacuations and in an ordinary day.

6.1.5. Night time evacuation during festival occasion

This scenario involving large number of visitors further emphasizes the need of detailed model of environment and complex agent functions, while those are necessary even for the former scenarios. The visitors are assumed to have no knowledge of the environment, and following others, with $g^{find_a_followee}$ and $g^{follow_an_agent}$, is their only way of reaching a safe place. That makes their visibility, which requires both detailed model of environment and complex agents, crucially important for the survival of visitors.

Just as in the previous night time evacuation scenario, it is assumed to be a full moon night, an earthquake has damaged the environment causing a power failure, and a tsunami is expected to arrive in 15 min. 18,000 visitors and 18,000 residents are assumed to be participating in the festival, which takes place in a 14 km² rectangular area shown in **Figure 17**. Agents participating the festival are distributed across the streets and open spaces, while another 39,000 residents are distributed over the whole domain. With full moon, 0.2 lx of lighting and 15 m sight distance are assumed, as in the former scenario. Another scenario with 30 m visibility is considered, in order to explore the mitigation measures of installing emergency lighting of 15 lx [14] at 30 m spacing which is equal to common street lighting. Maximum speeds of agents under these lighting conditions are set according to **Table 2**. Further, it is assumed that evacuees prefer to take safer paths, as in the previous scenario.

Figure 18 presents the results under the two lighting conditions considered. As seen, the low lighting conditions have significantly reduced the number of agents evacuated, compared that of an ordinary day. Further, it is observed that providing lighting of 15 lx significantly enhances the ability of the visitor agents to locate and follow others. An additional scenario with moon lighting without the earthquake induced damages is simulated to further explore the effect of lighting conditions. As seen in **Figure 18**, for this specific setting, the influence of lighting conditions is significantly higher than the earthquake induced damages.

6.2. Multi-modal evacuation with pedestrians and cars

In order to demonstrate the ability to perform large scale urban area evacuation simulations with sub-meter details considering the effect of car-pedestrian interactions a fictitious

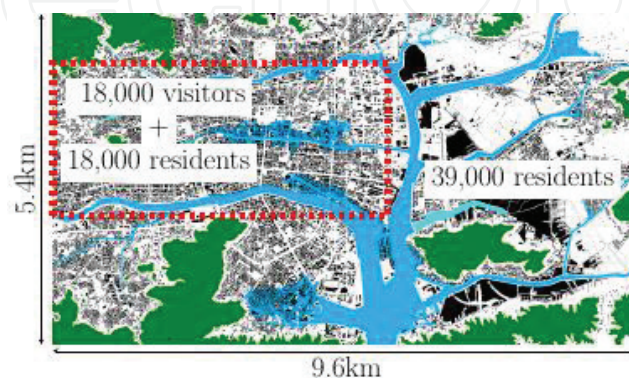


Figure 17. The area of study during the festival.

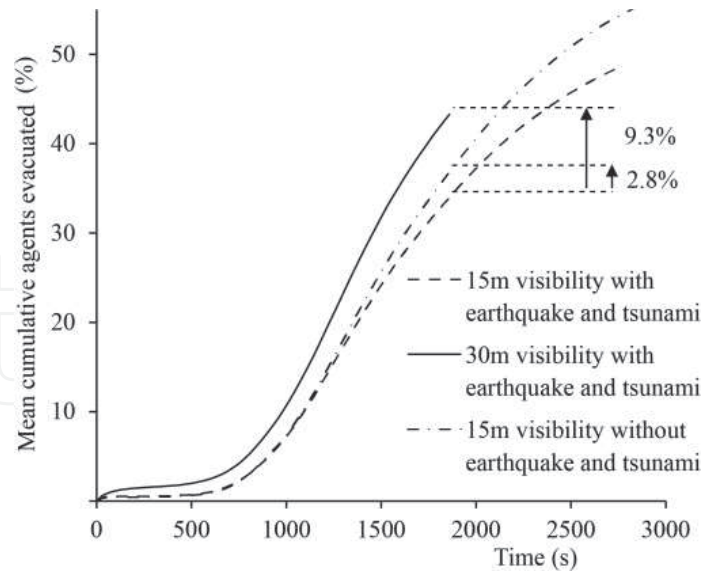


Figure 18. Simulation results under different visibility conditions.

tsunami-triggered evacuation in a coastal city of Japan is simulated. The effect of different strategies and mitigation measures are evaluated. The aim of this section is not to provide specific results to a real case scenario but to highlight the possibilities enabled by the introduction of mixed mode evacuation and interactions to the evacuation model.

6.2.1. Setting

The fictional setting is a $6 \times 6.5 \text{ km}^2$ area of a coastal city in Japan, see **Figure 19**. 40,000 evacuees are considered with the properties shown in **Table 3**. The tsunami arrival time is assumed to be 40 min as observed during the 2011 Great East Japan Earthquake and Tsunami which struck that region. The pre-evacuation time, the time it takes for an evacuee to start evacuating after the first earthquake shock, is assumed to follow a normal distribution.

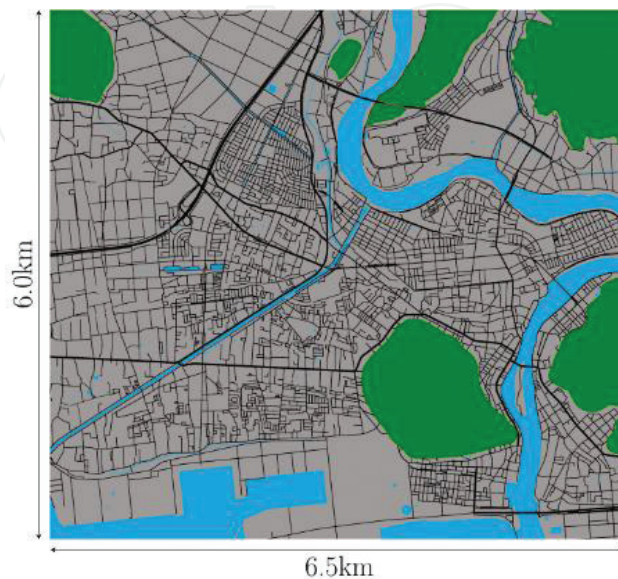


Figure 19. Environment for multimodal evacuation simulation.

	Younger than 50 years	Older than 50 years	
Percentage	50	50	Variable
Speed mean (m/s)	1.5	1.00	9.00
Speed S.D. (m/s)	0.4	0.4	2.00
Sight distance (m)	30	30	30
Pre-evacuation time mean (s)	900	900	900
Pre-evacuation time S.D. (s)	300	300	300

Table 3. Properties of the synthetic population used for the mixed mode evacuation scenarios.

The mean and standard deviation for this pre-evacuation time for pedestrians is obtained from literature [15]. A significant fraction of the population in this area is elderly, hence, the population is divided into two groups each constituting half of the population; *pedestrians fast* representing young people, and *pedestrians slow* representing elder people. The speed of each of each group is assumed to follow a normal distribution. Each vehicle is considered to carry two evacuees, representing a pessimistic usage of vehicles. Evacuees plan their evacuation route to the nearest evacuation areas.

6.2.2. Monte Carlo simulations

The instantiation of the synthetic population involves the initialization of random variables according to a given probability density function, for example, speed, pre-evacuation time, position in the domain. This allows to consider some of the uncertainties involved in real life. By relying on the law of large numbers, with a sufficient number of results, a stable average outcome can be provided. Furthermore, with an estimate of the results distribution, the robustness of the results of different scenarios can be compared. **Figure 20** shows the convergence of the standard deviation of the results with the number of draws/simulations.

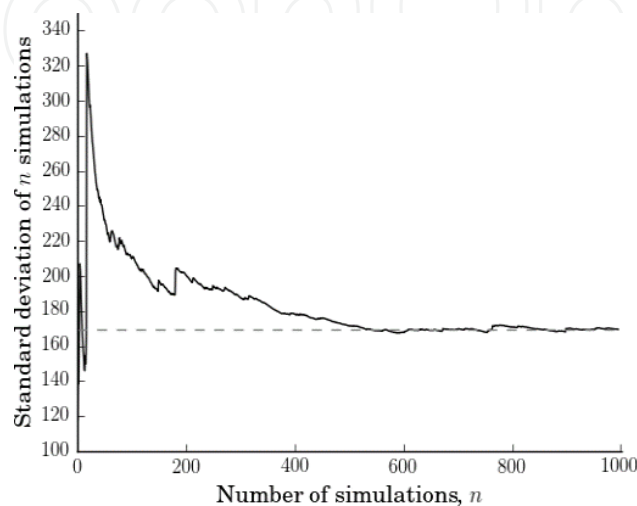


Figure 20. Convergence of the standard deviation of the results with the number of draws/simulations.

After about 600 simulations the standard deviation has already converged this contrasts with the pedestrian only simulations where convergence was achieved after 400 simulations, see **Figure 12**. **Figure 21** shows the mean and the standard deviation of the results of the cumulative number of agents evacuated with 1000 Monte Carlo simulations. The zoomed in box on the upper right corner shows a standard deviation of 0.42% in the throughput after 40 min, and in the lower right corner 0.29% after 25 min. Additionally, **Figure 22** shows the convergence of a more sensitive measure, the number of agents evacuated at each 10 s interval. The rest of the graphs present a single simulation result or the mean of 100 simulations; 600 simulations are not conducted for each scenario to reduce the computational resources used for this demonstration.

6.2.3. Indiscriminate use of cars

The first set of simulations explore a scenario where anyone, irrespective of their physical abilities, is allowed to use vehicles. **Figure 23**, compares the evacuation throughput with different percentages of evacuees using cars. It can be observed that as the percentage of evacuees using cars increases the total throughput after 40 min of evacuation decreases. There is an initial boost in the evacuation throughput especially during the first 25 min of evacuation.

Closer inspection shows the emergence of car queues along the roads connecting to some evacuation areas. This is considered the main reason for the throughput decrease.

6.2.4. People in need restriction

In order to evaluate the effect of selective usage of cars a scenario where only people in need are allowed to use cars is evaluated. People in need are defined as the evacuees having the slowest evacuation speed in the synthetic population.

The results obtained by restricting the use of cars can be seen in **Figure 24**. It can be seen that by applying this restriction an improvement in the total evacuation throughput of about 7% over the base scenario is achieved. Additionally, higher percentages up to 50% of the population can use cars without a significant impact in the total evacuation throughput. Moreover, it can be observed that the queue emergence remains as a problem.

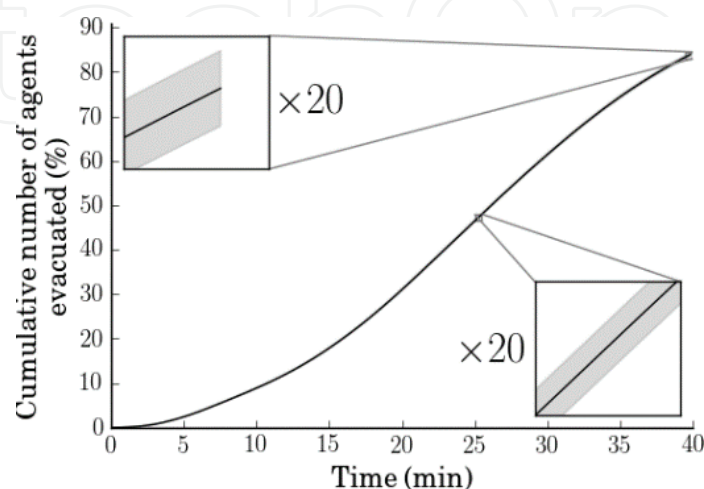


Figure 21. Time history of the evacuation, mean and the standard deviation of the cumulative number of agents evacuated with 1000 Monte Carlo simulations.

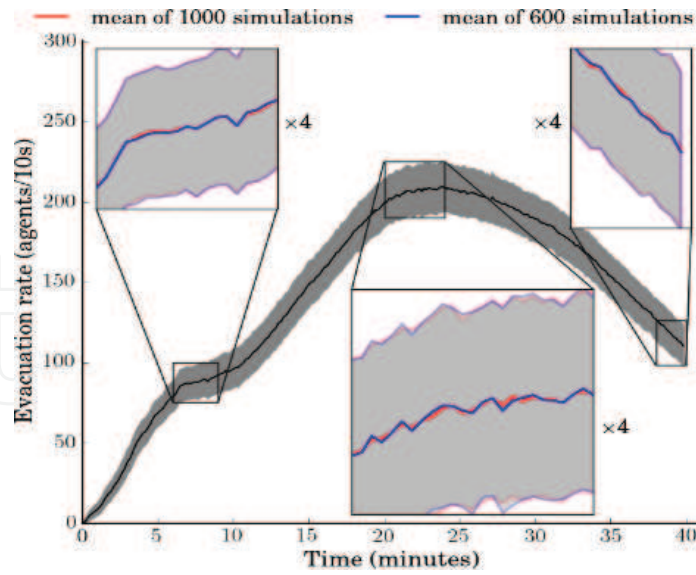


Figure 22. Convergence of the number of agents evacuated at each 10 s interval.

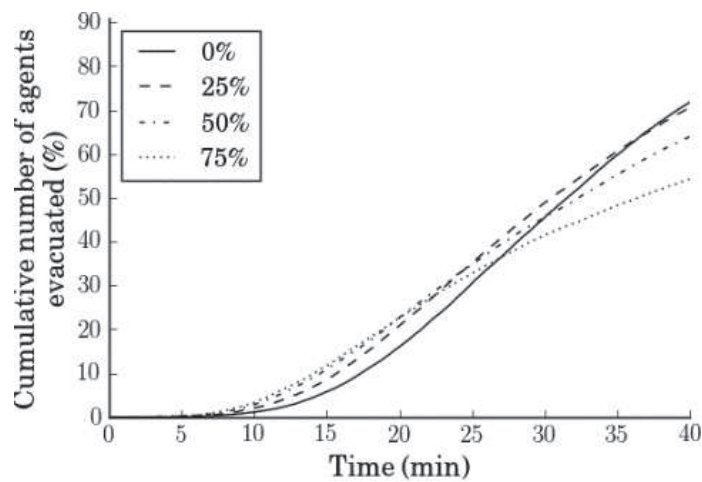


Figure 23. Time history of the evacuation varying the percentage of car usage. Anyone is allowed to use cars.

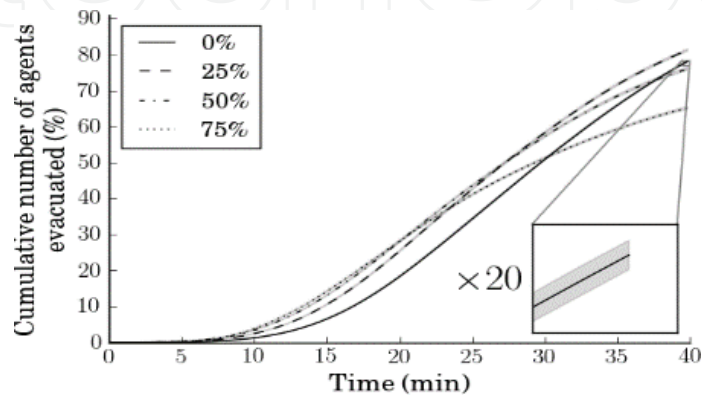


Figure 24. Time history of the evacuation varying the percentage of car usage. Only the elder people are allowed to use cars. 100 simulations mean and standard deviation.

7. Concluding remarks

This chapter provides a generic mathematical framework usable for the specification of other agent based systems providing a needed common language for comparison between models. The techniques and results of tuning the agents' interaction parameters are shown, showing the constrained validity of the model but also providing a data driven future for modelling agent's interactions. The results of scalability measures showing intra node strong scalability up to 8 threads and inter node strong scalability up to 2048 processes are shown. The techniques used for the domain decomposition and load balancing are generic enough to be easily extrapolated to other agent based systems. Finally, the demonstrative applications of the simulator show a usage case where the detailed models of environment and the detail of interactions are not only convenient but a necessity, highlighting the need of multi-agent systems considering the micro level interactions and details.

Author details

Leonel Aguilar, Maddegedara Lalith* and Muneo Hori

*Address all correspondence to: lalith@eri.u-tokyo.ac.jp

Earthquake Research Institute, The University of Tokyo, Tokyo, Japan

References

- [1] Leonel A, Lalith W, Hori M, Ichimura T, Tanaka S. A scalable workbench for large urban area simulations, comprised of resources for behavioural models, interactions and dynamic environments. *Lecture Notes in Computer Science*. 2014;**8861**:166-181
- [2] Van Den Berg, Jur, et al. "Reciprocal n-body collision avoidance." *Robotics research*. Springer Berlin Heidelberg, 2011. 3-19.
- [3] Aguilar. Enhancements and applications of a scalable multi-agent based large urban area evacuation simulator with emphasis on the use of cars [PhD Thesis]. The University of Tokyo; 2015
- [4] Weidmann U. *Transporttechnik der Fussgnger. Transporttechnische Eigenschaften des Fussngerverkehrs (Literturauswertung)*, Schriftenreihe des IVT Nr. 90, 2. Zurich; 1993
- [5] Dhingra, S. L., and Ishtiyag Gull. "Traffic flow theory historical research perspectives." *The fundamental diagram for traffic flow theory (2008)*: 45.
- [6] Melgar LEA, Lalith M, Ichimura T, Hori M. On the performance and scalability of an HPC enhanced multi agent system based evacuation simulator. In: *International Conference on Computational Science, ICCS2017*. 2017

- [7] Lalith W, Leonel A, Hori M, Ichimura T, Tanaka S. HPC enhanced large urban area evacuation simulations with vision based autonomously navigating multi agents. *Procedia Computer Science*. 2013;**18**:1515-1524
- [8] Aguilar L, Lalith M, Ichimura T, Hori M. Automatic evacuation management using a multi agent system and parallel meta-heuristic search. In: *International Conference on Principles and Practice of Multi-Agent Systems*. 2016
- [9] Hori M, Ichimura T. Current state of integrated earthquake simulation for earthquake hazard and disaster. *Journal of Seismology*. 2008;**12**(2):307-321
- [10] Galambos TV, Ellingwood B. Serviceability limit states: Deflection. *Journal of Structural Engineering, ASCE*. 1986;**112**(1):67-84
- [11] Xue M, Ryuzo O. Examination of vulnerability of various residential areas in china for earthquake disaster mitigation. In: *Proceedings of the 9th International Conference on Urban Earthquake Engineering/4th Asia Conference on Earthquake Engineering, Tokyo, 1931-1936*.
- [12] Baba, Toshitaka, et al. "Tsunami inundation modeling of the 2011 Tohoku earthquake using three-dimensional building data for Sendai, Miyagi Prefecture, Japan." *Tsunami events and lessons learned*. Springer Netherlands, 2014. 89-98.
- [13] Nichols TF, Powers TR. Moonlight and night visibility. U.S. Army Training Center Human Research Unit, Presidio of Monterey. 1964. URL <http://www.dtic.mil/dtic/tr/fulltext/u2/438001.pdf>.
- [14] Ouellette MJ, Rea MS. Illuminance requirements for emergency lighting. *Journal of the Illuminating Engineering Society*. 1989;**18**(1):37-42
- [15] Dulam R. Enhancement of multi agent simulation with smart agent interaction and high performance computing [Master Thesis]. The University of Tokyo; 2012

IntechOpen

